

N-terminal tagging of the dopamine transporter impairs protein expression and trafficking in vivo

Laura M. Vecchio, M. Kristel Bermejo, Pieter Beerepoot, Amy J. Ramsey, and Ali Salahpour
Department of Pharmacology, University of Toronto: Medical Sciences Building, Room 4302, 1
King's College Circle, Toronto, ON M5S 1A8, Canada

Abstract

The dopamine transporter (DAT) is the primary protein responsible for the uptake of dopamine from the extracellular space back into presynaptic neurons. As such, it plays an important role in the cessation of dopaminergic neurotransmission and in the maintenance of extracellular dopamine homeostasis. Here, we report the development of a new BAC transgenic mouse line that expresses DAT with an N-terminal HA-epitope (HAD-Tg). In this line, two copies of the HA-DAT BAC are incorporated into the genome, increasing DAT mRNA levels by 47%. Despite the increase in mRNA levels, HAD-Tg mice show no significant increase in the level of DAT protein in the striatum, indicating a defect in protein trafficking or stability. By crossing HAD-Tg mice with DAT knockout mice (DAT-KO), we engineered mice that exclusively express HA-tagged DAT in the absence of endogenous DAT (DAT-KO/HAD-Tg). We show that DAT-KO/HAD-Tg mice express only 8.5% of WT DAT levels in the striatum. Importantly, the HA-tagged DAT that is present in DAT-KO/HAD-Tg mice is functional, as it is able to partially rescue the DAT-KO hyperactive phenotype. Finally, we provide evidence that the HA-tagged DAT is retained in the cell body based on a reduction in the striatum:midbrain protein ratio. These results demonstrate that the presence of the N-terminal tag leads to impaired DAT protein expression in vivo due in part to improper trafficking of the tagged transporter, and highlight the importance of the N-terminus in the transport of DAT to striatal terminals.

Introduction

Dopamine is a catecholamine neurotransmitter involved in the regulation of a variety of functions including cognition, voluntary movement, mood, sleep, learning, motivation and reward (Salamone and Correa, 2012; Schultz, 2007; Tye et al., 2013). The dopamine transporter (DAT) is a transmembrane protein that regulates extracellular dopamine levels through reuptake of the released transmitter into presynaptic dopaminergic neurons, where it is either degraded or repackaged into vesicles for release (Caudle et al., 2007; Gainetdinov and Caron, 2003; Gainetdinov et al., 1998; Iversen, 1971; Nelson, 1998; Torres, 2006; Torres et al., 2003b). Levels of DAT on the plasma membrane largely determine the rate of dopamine clearance (Iversen, 1971; Melikian, 2004; Melikian and Buckley, 1999). Numerous proteins, including PICK1, HIC5, α -synuclein, syntaxin 1A and RACK, have

been shown to interact with DAT in heterologous cells, affecting targeting, total surface expression, and functional properties of the transporter (Carneiro et al., 2002; Foster et al., 2002; Lee et al., 1998, 2001, 2004, 2007; Melikian, 2004; Melikian and Buckley, 1999; Moron et al., 2003; Mortensen and Amara, 2003; Moszczynska et al., 2007; Torres et al., 2001; Vaughan et al., 1997). In light of these observations, DAT is considered to function as part of a protein complex rather than in isolation.

To study DAT protein–protein interactions and DAT trafficking in vitro, many studies utilize epitope tagged DAT. In these studies, the use of an epitope tag provides enhanced sensitivity and selectivity over the anti-DAT antibodies. For example, numerous past studies have reported that tagging DAT with an HA-epitope on the N-terminus does not disrupt protein expression or activity in heterologous cells (Hastrup et al., 2001; Khoshbouei et al., 2004; Salahpour et al., 2007; Torres et al., 2003a). N-terminal tagging of the DAT has therefore proven to be a useful strategy to study DAT biology in vitro. However the utility of N-terminal tagging has not been tested in vivo.

To test the potential functionality of an N-terminal tagged DAT in vivo, we developed a new transgenic mouse line by pronuclear injection of a modified bacterial artificial chromosome (BAC). Using a BAC containing the DAT locus and regulatory regions (Salahpour et al., 2008), we added a triple-HA tag onto the N-terminus of DAT by homologous recombination (Gong and Yang, 2005; Gong et al., 2002). We produced transgenic mice with two integrated copies of the modified HA-DAT BAC. The BAC transgenic approach successfully increased DAT message levels in the appropriate brain regions; however, DAT protein levels were not commensurate with message levels. Elimination of endogenous DAT protein, through intercross with DAT knockout (DAT-KO) mice, demonstrated that the HA-tagged DAT could only partially rescue the behavioral phenotype of DAT-KO mice. Mice expressing exclusively HA-tagged HA-DAT (DAT-KO/HAD-Tg) were shown to have approximately 8.5% striatal DAT relative to WT mice, whereas midbrain levels were detected at 27% relative to WT mice. Taken together, the biochemical and behavioral results of our study indicate a two-fold problem, where the N-terminal tagging of DAT impairs expression and trafficking of the transporter in vivo.

Results

Generation of transgenic mice expressing HA-tagged dopamine transporter

A two-step homologous recombination process (Gong et al., 2002) was used to modify a BAC in which the 40 kb murine DAT gene (*Slc6a3*) is flanked by 80 kb of flanking DNA both upstream and downstream of the gene. Previous work from our laboratory has demonstrated that this BAC contains the necessary sequence for proper spatiotemporal expression of the DAT (Salahpour et al., 2008). The targeting vector was designed to add three tandem copies of the HA-epitope to the N-terminus of the DAT (Supplementary Fig. 1). Following two rounds of homologous recombination, properly modified HA-DAT BAC clones were identified by PCR. A germline-transmitting transgenic founder line was generated by pronuclear injection of C57Bl/6J embryos and was identified by PCR genotyping. Subsequent breeding confirmed that the 3HA-DAT BAC integrated in a single

locus and was autosomally transmitted. Transgenic mice were termed HAD-Tg (*HA-DAT* Transgenic).

The copy number of HA-DAT BAC integrants in the genome was determined by quantitative PCR of genomic DNA using primers specific for the *Slc6a3* sequence. The rate of amplification of DAT amplicons was compared to that of a reference gene, *Tfrc*, using genomic DNA from wild type (WT) and HAD-Tg mice. As shown in Fig. 1A, there is an estimated 2-fold increase in DAT copy number in HAD-Tg mice as compared to WT mice, which is indicative of two integrated copies of HA-tagged DAT BAC in addition to the two endogenous alleles. We next evaluated the levels of DAT mRNA in HAD-Tg mice compared to WT animals using reverse-transcription quantitative PCR (Fig. 1B). To ensure that measurements reflected the amount of DAT mRNA in dopaminergic cells, DAT amplicons were normalized to amplicons of tyrosine hydroxylase (TH), a marker of dopamine neurons in the midbrain. Midbrain tissue samples from HAD-Tg mice have a 47% increase in DAT mRNA levels relative to WT mice ($p = 0.011$). This result indicates that there is increased DAT mRNA in HAD-Tg mice and that the addition of the N-terminal HA tag does not interfere with the transcription of the DAT gene.

HA-DAT is expressed in regions endogenously expressing DAT

The spatial pattern of expression of HA-DAT within the transgenic line was examined by immunohistochemistry. As shown in Fig. 2, expression of HA-DAT is restricted to neurons that express DAT endogenously, demonstrated by the co-localization of HA and DAT immunoreactivity in the striatum (Fig. 2A) and the substantia nigra/ventral tegmental area of the midbrain (Fig. 2B). Furthermore, immunoreactivity for HA is undetected in regions where native DAT protein is not expressed. Immunohistochemistry of sagittal sections further demonstrates that HA-tagged DAT is expressed along the dopaminergic nigrostriatal and the mesolimbic pathways, in a pattern that mirrors endogenous DAT (Fig. 2C).

One potential explanation for the lack of increase in DAT protein is that the presence of the HA-tag may prevent antibody binding to the DAT, particularly since the antibody used in Fig. 3 is against the N-terminal sequence of the DAT. To ensure that the lack of detectable DAT levels is not due to the antibody used, striatal protein samples from WT and HAD-Tg mice were probed with both an N-terminal DAT antibody as well as a C-terminal DAT antibody. As shown in Fig. 4, there is no significant difference in DAT levels between WT and HAD-Tg mice using either the N-terminal or C-terminal antibody, indicating that the apparent paucity of HA-DAT is not an artifact of antibody detection. Importantly, there is no significant difference when comparing the N-terminal and C-terminal DAT signal (N-terminal/C-terminal DAT) within the same animal (Fig. 4). Moreover, the DAT revealed by both the N-terminal and C-terminal antibodies represents mature DAT, approximately 70 KDa in weight (Supplementary Fig. 2).

N-terminal tagging of the dopamine transporter interrupts expression in the striatum

To further investigate the amount of DAT protein that is produced from the HA-DAT transgene, we intercrossed HAD-Tg mice with DAT-KO mice (Giros et al., 1996) to remove all endogenous DAT; these mice were termed DAT-KO/HAD-Tg. We measured striatal DAT

protein levels by western blot from DAT-KO/HAD-Tg mice, WT mice, and also DAT-HET mice possessing one allelic copy of endogenous DAT (Fig. 5A). As expected, DAT-HET mice had approximately half the striatal DAT protein relative to WT mice (41%). Importantly, the level of DAT in the striatum of DAT-KO/HAD-Tg mice was only 8.5% that of WT mice (Fig. 5B). To determine whether the HA-DAT present in the striatum was functional, we performed dopamine uptake experiments from striatal synaptosome preparations. The level of $^3\text{H}[\text{DA}]$ uptake from DAT-KO/HAD-Tg mice was approximately 12% of WT when subtracting background uptake from DAT-KO tissue (Fig. 5C). These results reveal that despite the 50% increase in DAT mRNA (Fig. 1), very little HA-DAT protein is in fact present in the striatum of transgenic mice. Importantly, midbrain DAT levels in DAT-KO/HAD-Tg mice were 27% of levels found in WT midbrain (Fig. 6). Therefore impaired expression of HA-tagged DAT is more profound in the striatum than the midbrain of DAT-KO/HAD-Tg mice.

HA-tagged DAT expression partially rescues hyperactivity of DAT knockout mice

Next, we evaluated whether the HA-tagged DAT was functional by examining whether it could rescue the behavioral phenotype of mice lacking endogenous DAT. DAT-KO mice exhibit distinct behavioral phenotypes that include hyperlocomotion and impaired habituation to novel environment (Fukushima et al., 2007; Gainetdinov et al., 1999a; Giros et al., 1996). By crossing DAT-KO mice with HAD-Tg mice, we assessed whether the hyperactivity in DAT-KO mice could be normalized by the expression of the transgene. If so, this would indicate that the HA-tagged DAT is functional. Fig. 7 shows that expression of HA-tagged DAT in DAT-KO mice significantly reduced the total distance traveled by the animals in 120 min (from 26 470 cm to 8583 cm, $p < 0.0001$, Student's t-test). Therefore, the HA-tagged DAT transgene is sufficient to partially rescue the hyperactivity displayed by DAT-KO mice. Interestingly, the locomotor activity of DAT-KO/HAD-Tg mice is significantly higher than that of WT animals, indicating that the HA-tagged DAT can only partially rescue the DAT-KO hyperactive phenotype (Fig. 7; $p < 0.0001$, t-test). This is consistent with western blots showing that the striatal levels of HA-tagged DAT are less than 10% of normal DAT levels.

Response to amphetamine is attenuated in mice expressing only HA-tagged DAT

The locomotor response to amphetamine is directly proportional to striatal DAT levels, as previously shown in both DAT over-expressing and several DAT-KO mice studies (Gainetdinov et al., 1999b; Salahpour et al., 2007, 2008). Mice lacking DAT or expressing low-levels of DAT display reduced rather than increased activity in response to amphetamine (Cagniard et al., 2014; Gainetdinov et al., 1999a, 1999b; Zhuang et al., 2001). Both wildtype and HAD-Tg mice display hyperlocomotion with 2.0 mg/kg of amphetamine administration (Fig. 8 and Supplementary Fig. 3). However, mice that only express HA-tagged DAT (DAT-KO/HAD-Tg) display a reduction in activity after administration of amphetamine that resembles the behavioral response of DAT-KO mice (Fig. 8 and Supplementary Fig. 3).

N-terminal HA tagging of DAT interrupts transport from the midbrain to striatum

In a direct comparison between WT and HAD-Tg mice, transgenic mice showed no increase in DAT levels in neither the midbrain nor the striatum (Fig. 4). In addition, HAD-Tg mice

lacking endogenous DAT only express 8.5% of normal striatal DAT levels (Fig. 5). To determine the reason why so little HA-tagged DAT is detected in the striatum, we examined whether the HA epitope interfered with targeting of DAT from the dopamine cell bodies in the midbrain to the terminals in the striatum. We performed western blots comparing striatal to midbrain protein using regional samples from the same mice. First, we established the ratio of DAT that is normally present in the striatum versus the midbrain of WT mice. Then, using samples from DAT-KO/HAD-Tg mice, we established the ratio of HA-tagged DAT present in the striatum versus midbrain using anti-HA antibody (Fig. 9A–B). The striatum:midbrain ratio of HA-tagged DAT is approximately 44% lower than the ratio of endogenous DAT in WT mice. In WT mice, the striatum:midbrain ratio of DAT is approximately 5.24, whereas in HAD-Tg mice the striatum:midbrain ratio of HA-tagged DAT is only 2.92 ($p = 0.001$, t-test) (Fig. 9C).

Results obtained from the western blot densitometry ratio analysis of HA-tagged DAT (striatum to midbrain) were recapitulated using immunohistochemistry. In sagittal sections, we demonstrated that the ratio of HA-DAT in the striatum compared to midbrain in transgenic mice is significantly reduced as compared to the ratio of DAT in the striatum to midbrain of wildtype mice (0.96 and 1.80, respectively; $p = 0.0002$) (Fig. 10).

Both western blot and immunohistochemistry techniques revealed that the striatum:midbrain ratio of wildtype DAT is approximately 1.8 times higher than the ratio of striatal:midbrain HA-tagged DAT. These results suggest a reduction in the proportion of HA-tagged DAT that reaches the striatum from the midbrain compared to endogenous DAT, and indicate that the addition of the HA-tag at the N-terminus interferes with targeting and/or transporting of DAT from the midbrain to axonal terminals.

Discussion

In this study, we successfully created BAC transgenic mice expressing an HA-epitope tagged DAT. We showed that despite a 50% increase in DAT mRNA, there was no discernable increase in total DAT protein in the striatum or midbrain of the transgenic animals (Fig. 3). The reduced levels of DAT in the HA transgenic animals could be due to several things. First, we show that there is a reduction in DAT expression in the midbrain of HA-transgenic animals, indicating that there may be either an issue with protein expression or increased degradation of DAT within the midbrain. However, the reductions of DAT in the midbrain are less than those in the striatum, 75% vs 90% respectively. Therefore expression alone cannot fully account for the reductions that we observe in the striatum, indicating that there is also a deficit in trafficking of the transporter from the midbrain to the striatum. Indeed, this would be consistent with our observations indicating that ratio of striatum: midbrain DAT protein is lower for the HA-DAT compared to the WT protein. An alternate explanation for reduced DAT levels in the striatum would be increased endocytosis and degradation of the transporter. Indeed, there is evidence that the N-terminus of DAT contains domains that negatively regulate endocytosis (Sorkina et al., 2009). It is possible that insertion of the HA epitope in an in vivo setting masks these domains, resulting in reduced accumulation of DAT in the terminals. All together, our results show that N-terminal tagging of the DAT impairs

both protein expression (either through enhanced degradation or reduced translation) as well as affecting trafficking of the protein.

To assess the expression and functionality of HA-DAT, we crossed the HAD-Tg mice with DAT-KO mice to generate animals that only express the tagged version of DAT. Several lines of evidence indicate that the HA-DAT protein that is present appears to be fully functional. First, uptake studies demonstrated 12% DAT activity in HA-DAT mice compared to wildtypes. Second, expression of the HA-DAT was able to partially rescue the hyperlocomotor phenotype of DAT-KO mice. Third, the behavioral response to amphetamine was more consistent with a 90% downregulation rather than a complete absence of DAT. Indeed, while amphetamine is a stimulant in wildtype mice, it reduced activity in mice expressing only HA-tagged DAT. A similar result was previously reported in DAT knockdown animals that only express 10% of wildtype levels (Cagniard et al., 2014; Zhuang et al., 2001). Notably, the “calming” effect of amphetamine was more substantial in DAT-KO mice than that in animals only expressing HA-DAT, indicating the presence of some functional DAT in HA-tagged animals. Again this supports the conclusion that the N-terminal tag does not interfere with DAT function but instead affects protein levels and trafficking.

Our results can be considered in the context of several studies that have quantified behavioral phenotypes of mice with varying levels of DAT. For example, two different knockdown lines have been described. In one line, DAT levels are 35% (Rao et al., 2013), while in the other, DAT levels are 10% of wildtype (Zhuang et al., 2001). It has been shown that both knockdown lines display hyperactivity proportional to the extent of DAT knockdown. Importantly, knockdown animals that express 10% normal DAT levels display reduced activity in response to amphetamine, similar to what we observed in our HA-DAT line (Cagniard et al., 2014; Rao et al., 2013; Zhuang et al., 2001). Behaviors of DAT knockdown animals are similar but less severe than what is observed in DAT knockout mice (Gainetdinov et al., 1999a; Rao et al., 2013; Zhuang et al., 2001). Furthermore, DAT heterozygous mice that express 50% of normal DAT levels have no basal hyperactivity and are stimulated rather than calmed with amphetamine treatment (Fukushima et al., 2007; Salahpour et al., 2007). The behavioral profile of our mice that only express HA-DAT (basal hyperactivity and amphetamine calming) mirrors DAT knockdown phenotypes rather than DAT heterozygotes.

Numerous in vitro studies have used N-terminal tagged DAT in heterologous cell systems, and in those studies DAT function appears to be unaffected by the tag. Our studies also indicate that the tag does not impair the proton/DA exchange property of the DAT in vivo. However we do show that trafficking of DAT from the midbrain to the striatum is impaired. This impaired trafficking may be the result of the epitope interrupting important protein-protein interactions that determine DAT localization in vivo. Indeed, the N-terminus of DAT is a site of phosphorylation, which is believed to play an important role in trafficking (Foster et al., 2002, 2006; Vaughan, 2004; Vaughan et al., 1997). N-terminal residues have also been shown to negatively regulate DAT endocytosis (Sorkina et al., 2009). Furthermore, the amino terminus is a site of direct interaction between DAT and both syntaxin 1A and RACK1 (Carvelli et al., 2004, 2008; Cervinski et al., 2010; Lee et al., 2004). The interaction

with syntaxin – possibly, via the formation of a syntaxin-RACK1-DAT complex – has been suggested to mediate DAT trafficking through modulation of DAT phosphorylation (Foster et al., 2006; Lee et al., 2004). Furthermore, the interaction of syntaxin and DAT has also been demonstrated in DA neurons in *Caenorhabditis elegans*. In that study, the addition of an N-terminal GFP to DAT interrupted the syntaxin–DAT association and resulted in disruptions in thrashing behavior (Carvelli et al., 2008). Our study further supports the notion that the N-terminus is an important site for protein interactions, and that modification of this site disrupts DAT function and trafficking in vivo.

The C-terminus of DAT has also been shown to be important for trafficking as it contains a PDZ-binding sequence that interacts with the protein PICK1. This interaction was originally proposed to be responsible for the export of DAT from the endoplasmic reticulum (ER) in heterologous cell lines (Miranda et al., 2004; Torres et al., 2001). However, later studies demonstrated that while surface targeting of DAT does involve the C-terminus, the PDZ domain is neither necessary nor sufficient for DAT surface expression in heterologous cells (Bjerggaard et al., 2004). A recent study showed that the PDZ-domain interactions are critical for membrane distribution of DAT on dopaminergic neurons, and a mutant DAT protein with a disrupted PDZ-binding motif resulted in a 90% reduction of DAT in striatal terminals (Rickhag et al., 2013). Additionally, disrupting the PDZ-domain in mutant mice resulted in an attenuated locomotor response to amphetamine, indicating a profound loss of striatal DAT (Rickhag et al., 2013). However, while the C-terminal PDZ domain was shown to be involved in distribution of striatal DAT in vivo, PICK1 is not believed to be involved in this process, as PICK1 knockout mice were shown to have normal distribution of DAT in both the midbrain and striatum (Rickhag et al., 2013).

Our study provides the first evidence that the N-terminus of DAT is also involved in the expression of DAT in striatal terminals in mice. The lack of expression of HA-DAT cannot be explained by site of insertion of the DAT BAC or improper transcription of the transgene, since a 50% increase in DAT mRNA was detected in HAD-Tg mice. Therefore, our data suggests that tagging DAT on the N-terminus affects protein expression efficiency as well as interrupting transport of DAT, particularly at neuronal terminals. Importantly, we showed that the ratio of striatal to midbrain HA-DAT is reduced by up to 47% compared to the normal ratio of striatal to midbrain DAT, as demonstrated by both immunohistochemistry and western blot (Figs. 9 and 10). The N-terminus of DAT has been previously linked to amphetamine-induced efflux of DA (Khoshbouei et al., 2004) and has been identified as a site of phosphorylation (Cervinski et al., 2010; Foster et al., 2002, 2006), as well as a site of ubiquitination leading to transporter endocytosis (Miranda et al., 2007). Our study has provided a foundational support for further investigation into the possible role of the N-terminus of DAT in the targeting and transport of DAT to neuronal terminals in vivo.

Conclusion

The HA-tag is considered ideally suited for tagging proteins because of commercially available, high-affinity antibodies. N-terminally HA-tagged DAT has been successfully expressed in mammalian cells and has been used in several studies (Hastrup et al., 2001, 2003; Khoshbouei et al., 2004; Salahpour et al., 2007; Torres et al., 2003a). Additionally,

knock-in mice with an HA-tag in the second extracellular loop of DAT have also been generated as a tool for studying endogenous trafficking and subcellular localization of DAT (Rao et al., 2012; Sorkina et al., 2006). Because of the success of these past models, we created transgenic mice possessing a triple HA-tag on the N-terminus of DAT. Our characterization of these animals clearly shows that, while tagging the N-terminus may not result in a disruption of DAT expression in heterologous cells, the same is not true in vivo. In this study, the presence of the N-terminal HA-tag leads to impaired protein expression despite increased mRNA levels, in part due to reduced protein expression as well as impaired trafficking of the tagged-transporter to striatal terminals. These results highlight the importance of the N-terminus for trafficking and expression of DAT in vivo. Therefore, further studies are required to decipher the precise role of DAT N-terminus for proper expression and targeting of the transporter in vivo.

Experimental methods

Animals

All experiments used age- and gender-matched WT and transgenic (HAD-Tg) littermate mice aged 3–5 months and maintained on a C57Bl/6J genetic background. Mice were housed on a 12 hour light-dark cycle and food and water was provided ad libitum. Procedures conformed to the recommendations of the Canadian Council on Animal Care and the National Institutes of Health guidelines for the care and use of animals, with protocols reviewed and approved by the University of Toronto Faculty of Medicine and Pharmacy Animal Care Committee.

Generation of HA-DAT mice

A BAC containing the murine DAT locus was obtained from Genome Sciences. The DAT BAC4 clone was chosen for pronuclear injection because it contains the required regulatory and promoter sequences necessary for proper DAT spatial and temporal expression (Salahpour et al., 2008). In addition, the DAT BAC also contains a gene encoding chloramphenicol resistance. Two-step homologous recombination (Gong et al., 2002) was used to modify the BAC, which enabled the addition of an HA tag consisting of three tandem copies of the epitope to the N-terminus of the murine DAT (Supplementary Fig. 3). A PLD53 SC-AB shuttle vector (Gong et al., 2002) was used to insert the HA epitope, flanked by homology regions A and B (Supplementary Fig. 3B). Homology arm A was prepared with the following sequences: 5' *ggcgcgcctctgtacctgtctgt* and 3' *accagatcctcagggccatgggtagacgggagcccagggaag*. Homology arm B was prepared with: 5' *gatgaagaatctgagagtgactgaggctaaagagcccaatgctgtg* and 3' *ttaattaagcatcttctctcctcagtt*. Supplementary Fig. 3C depicts the co-integration of the shuttle vector into the DAT BAC via homologous combination of region A (step one). The correct co-integrants contained both the BAC and the vector sequences, and were selected by growth in 20 µg/ml chloramphenicol (Sigma, C3175) and 50 µg/ml ampicillin (BioShop, AMP20125) and verified by PCR of miniprep DNA (Gong et al., 2002). The recombinant clone was subsequently grown in liquid media (LB with 20 µg/ml chloramphenicol and approximately 4.5% sucrose) to select for a second homologous recombination event that eliminates the PLD vector (Gong et al., 2002) (Supplementary Fig. 3D). Clones harboring the resolved

BACs were selected by growth on plates with 20 µg/ml chloramphenicol and 4.5% sucrose media, and the correct recombination event was verified by PCR of miniprep DNA.

The BAC DNA was isolated using the Clontech BAC preparation kit and resuspended at 2 ng/µl in injection buffer (0.03 mM spermine/0.07 mM spermidine). The modified BAC was used for pronuclear injection of C57BL/6J embryos. Injections were performed by the Duke Transgenic Mouse Facility. One transgenic positive founder was identified by PCR-based genotyping using primers that amplify BAC vector sequence (forward, 5' - *gcatcagccagcgcagaaatatttcc*; reverse, 5' - *gatacttcggtatcgaccagctgc*) (Salahpour et al., 2008). This founder was used to establish the transgenic line used for this study (HAD-Tg).

Quantitative PCR

Genomic DNA—Genomic DNA was isolated from tail biopsy after proteinase K digestion and isopropanol precipitation (Ballester et al., 2004; Burkhart et al., 2002). DNA was further cleaned using a chloroform–ammonium acetate method. Optical density was measured at 260/280 nm and dilutions of both 20 ng/ul and 5 ng/ul dilutions were prepared from each DNA sample. The following primers were used to amplify DAT genomic sequence: forward: 5' - *gggcagcatccactagataaa*, reverse: 5' - *acactctctagactaccatcc*, and amplicons were measured relative to those of the reference gene, *Tfrc* (forward: 5' - *cagtcacagggttgctaata*, reverse: 5' - *atcacaacctcacatgtaact*). At both dilutions of the DNA, quantitative PCR was used to determine total allelic copy number of DAT including both native alleles as well as copies of the transgenic HA-tagged DAT, as previously described (Ballester et al., 2004; D'Haene et al., 2010; Shepherd et al., 2009), using the Applied Biosystems 7500 Real-Time PCR System. Relative quantification of gene targets was obtained using the GoTaq® qPCR Master Mix (Promega, Fitchburg, WI, USA). The PCR cycle consisted of 1 repeat at 50 °C lasting 2 min, 1 repeat at 95 °C for 10 min, 40 repeats at 95 °C for 15 s and ended at 60 °C for 1 min. Analysis of gene copy number was based upon the 2^{-CT} method, as previously described (Livak and Schmittgen, 2001; Pfaffl, 2001; Schmittgen and Livak, 2008). Copy number was determined by normalizing CT of transgenic mice to those with wildtype controls, whom are known to possess two copies of the target gene.

mRNA—Following sacrifice by cervical dislocation, brains were removed and frozen in 2-methylbutane over dry ice. Whole brains were stored at -80 °C and subsequently used for RNA extraction. To obtain total RNA from tissues, midbrain regions were microdissected from a 1 mm coronal section, were homogenized in cold Tri-Reagent (BioShop), and processed as described (Hu et al., 2009). Optical density readings at 260/280 nm were used to determine the quality and concentration of RNA. For reverse transcriptase PCR, 300 ng of RNA was used to obtain complementary DNA using SuperScript III Reverse Transcriptase (Invitrogen) following the manufacturer's instructions. As before, relative quantification of gene targets was obtained using the GoTaq® qPCR Master Mix on the Applied Biosystems 7500 Real-Time PCR System. Phosphoglycerate kinase 1 (PGK1) was used as the reference gene (forward primer: 5' - *ggccttcgacctcaggtgt*, reverse primer: 5' - *gtccaccctcatcacgaccg*). DAT (forward primer: 5' - *ggcctgggctcaacgacac*, reverse primer: 5' - *ggtgcagcacaccagctcaa*) and TH (forward primer: 5' - *cgggcttctgaccaggcg*; reverse primer: 5' - *tgggaattggctcacctgct*) were used as the target genes. Target genes were relatively

quantified using the Ct method, and were normalized to PGK1 (Livak and Schmittgen, 2001; Pfaffl, 2001; Schmittgen and Livak, 2008). Data are represented as the ratio of the normalized expression of DAT to TH.

Western blot

The midbrain and the striatum were dissected from freshly harvested brains. Brain samples were mechanically homogenized in RIPA buffer (50 mmol/l Tris-HCl, pH 7.4/150 mmol/l NaCl/1% Nonidet P-40/0.5% sodium deoxycholate/0.1% SDS; Sigma) plus protease inhibitor mixture (Roche 1873580), and protein concentration was measured by using a BCA protein assay kit (Thermo Scientific). Protein extracts (25 µg for the striatum, 60 µg for the midbrain) were separated by 10% SDS/PAGE and transferred to nitrocellulose membranes. Blots were blocked with LI-COR blocking buffer for 1 h (LIC-927-40100), and immunostained overnight at 4 °C with primary antibodies: N-terminal rat anti-DAT (1:750 dilution; Chemicon MAB369) and mouse anti-GAPDH (1:2000, Sigma G8795). After washing, protein bands were revealed with fluorescence-labeled secondary antibodies donkey anti-rat IRdye 800CW and donkey anti-mouse IRdye 800CW (1:5000 dilutions; Rockland, 612-732-120 and 610-731-002, respectively). Membranes were then stripped, blocked in 5% milk powder for 1 h and incubated overnight at 4 °C with the primary antibodies rabbit anti-HA (1:1000 dilution; Bethyl A190-108A) and rabbit anti-TH (1:3000 dilution; Millipore, AB152). The protein bands were then revealed with a goat anti-rabbit Alexa Fluor (AF) 680 secondary antibody (1:5000 dilution; Invitrogen, A21076).

In a separate set of experiments, an additional rabbit anti-DAT primary antibody, selective for the C-terminus, was incubated overnight in LI-COR buffer (1:750 dilution; Santa Cruz, C-20, SC-1433) at the same time as the N-terminal anti-DAT and revealed with goat anti-rabbit AF680 (1:5000 dilution). The membrane was then stripped and probed for HA and TH. To ensure that there was no cross-reactivity between N- and C-terminal antibodies, two separate gels were also run; one was probed only with N-terminal rat anti-DAT and the other, only with C-terminal goat anti-DAT. Both of these membranes were also probed for HA, TH and GAPDH as previously described. These membranes were left uncut to demonstrate that only one species of DAT was detected by both antibodies, which ran at 70–75 KDa (Supplementary Fig. 2). Densitometric analyses were conducted using Image Processing and Analysis in Java (ImageJ) software (<http://rsb.info.nih.gov/ij/index.html>).

Immunohistochemistry

Mice were anesthetized with avertin (250 mg/kg) prior to perfusions. Mice were intracardially perfused with phosphate buffered saline (PBS) at a flow rate of 80 ml·h⁻¹ for 2 min, followed by 4% paraformaldehyde in PBS for 8 min. The brains were removed and stored at 4 °C in 4% paraformaldehyde in PBS overnight, then transferred to a 30% sucrose solution for cryoprotection, for 48 h at 4 °C. Tissue was then blocked in freezing media HistoPrep (Fisher Chemical, SH75-125D) and cut in 50 µm coronal and sagittal sections using a cryostat (Leica, CM1510).

Floating sections were quenched in 0.5% sodium borohydride in PBS, washed, and blocked for 2 h at room temperature [10% normal goat serum (NGS), 0.75% bovine serum albumin

(BSA), 0.1% Triton-X, in PBS]. Blocking was followed by an overnight incubation at 4 °C that contained rat anti-DAT (1:200 dilution) and rabbit anti-HA (1:2000 dilution) in antibody solution (10% NGS, 0.75% BSA, and 0.01% Triton-X in PBS). Sections were then washed in chilled PBS, and incubated with secondary antibodies anti-rat IRdye 800 (1:1000 dilution) and anti-rabbit AF680 (1:4000 dilution) for 1 h at room temperature. The slices were then mounted with Thermo Scientific Aqua-Mount Slide Mounting Media (Thermo Scientific, 143905) and scanned at high resolution with the LI-COR system, at an offset of 0.85 mm.

In a separate set of experiments, 40 µm sagittal sections were cut and stained as described above. Densitometric analyses were made to compare HA immunoreactivity of the striatum to midbrain in transgenic mice (Supplementary Fig. 4). In a similar way, densitometry was used to compare DAT immunoreactivity of the striatum to midbrain in wildtype mice. Striatum:midbrain ratios were calculated accordingly.

Locomotor analysis

Locomotor activity was assessed in automated locomotor activity monitors (Accuscan Instruments). Mice were placed into the activity monitor chamber (20 cm × 20 cm) and measured at 'baseline' conditions for 120 min. Locomotor activity was measured in terms of the total distance covered and stereotypic behaviors, collected in 5 minute bins.

Rescue of DAT-KO mice

HAD-Tg mice were crossed to DAT knockout mice to verify whether HA-DAT can rescue the DAT-KO phenotype. With regard to endogenous DAT, these mice could be WT, missing one DAT allele (heterozygous, DAT-HET), or missing both DAT alleles (homozygous, DAT-KO). In addition, they either possessed no HA-tagged DAT (HAD nTg) or were transgenic (HAD-Tg). Mice of six distinct genotypes were compared (described DAT genotype/HAD genotype): WT/HAD-nTg; WT/HAD-Tg; DAT-HET/HAD nTg; DAT-HET/HAD-Tg; DAT-KO/HAD-nTg; and DAT-KO/HAD-Tg. WT is used to refer to WT/HAD-nTg mice. Baseline locomotor activity was assessed as the total distance traveled in 120 min. For these studies, we compared the activity of DAT-KO mice possessing HA-DAT to non-sibling DAT-KO mice. Protein analyses were made by western blot using striatal (25 µg) and substantia nigra (60 µg) samples.

Amphetamine challenge

The locomotor activity of mice was recorded, as previously described at baseline for 120 min. Following baseline recording, mice were injected with a dose of 2 mg/kg amphetamine and recorded for 90 min.

Preparation of striatal synaptosomes

Fresh crude striatal synaptosomes were prepared according to the procedure outlined by Javitch et al. (1985) with modifications. Mice were sacrificed by cervical dislocation after which the brain was removed rapidly and placed in ice-cold PBS for 2 min. Subsequently, the striatum was dissected on an ice-cold surface from 1 mm thick coronal slices. The striatum from one mouse was used for each synaptosome preparation, and tissue was homogenized in 0.25 ml ice-cold 0.3 M sucrose in a 1.5 ml centrifuge tube using a

polypropylene pestle. The homogenate was diluted 1:4 in 0.3 M sucrose and centrifuged at $1000 \times g$ for 10 min at 4 °C. The supernatant was then removed and centrifuged at $12,000 \times g$ at 4 °C for 20 min. The resulting pellet was resuspended in uptake buffer, after which protein concentration was determined by BCA assay (Biorad) The solution was subsequently diluted in uptake buffer to 1 $\mu\text{g}/\mu\text{l}$ for uptake experiments.

Radiolabeled DA uptake into striatal synaptosomes

25 μl of striatal synaptosome preparation was added to tubes containing 450 μl uptake buffer (4 mM Tris-HCl, 6.25 mM HEPES, 120 mM NaCl, 5 mM KCl, 1.2 mM CaCl₂, 1.2 mM MeSO₂, 5.6 mM D-glucose, 0.5 mM ascorbic acid, final pH 7.1) The solution was incubated for 30 min, after which a mixture of 1/8 hot/cold dopamine was added (0.125 μM hot dopamine (2.8125 μCi , 45 Ci/mmol); 0.875 μM cold dopamine). After 5 min of incubation, 5 ml of cold uptake buffer was added to stop uptake followed by filtration through Whatman GF/B glass-fiber filters. The filters were washed twice with 5 ml of 50 mM Tris-HCl and analyzed for tritium radioactivity in a PerkinElmer Tri-Carb 2900TR liquid scintillation counter. Nonspecific uptake was determined in the presence of 100 μM of cocaine. Assays were performed in triplicate for each synaptosome preparation and the average of the triplicate was used for subsequent data analysis.

Statistics

Data are reported as means \pm SEM. Statistical significance was evaluated by two-tailed t test, one-way and two-way ANOVA, as appropriate.

Supplementary Material

Refer to Web version on PubMed Central for supplementary material.

References

- Ballester M, Castello A, Ibanez E, Sanchez A, Folch JM. Real-time quantitative PCR-based system for determining transgene copy number in transgenic animals. *Biotechniques*. 2004; 37:610–613. [PubMed: 15517974]
- Bjerggaard C, Fog JU, Hastrup H, Madsen K, Loland CJ, Javitch JA, Gether U. Surface targeting of the dopamine transporter involves discrete epitopes in the distal C terminus but does not require canonical PDZ domain interactions. *J Neurosci*. 2004; 24:7024–7036. [PubMed: 15295038]
- Burkhart CA, Norris MD, Haber M. A simple method for the isolation of genomic DNA from mouse tail free of real-time PCR inhibitors. *J Biochem Biophys Methods*. 2002; 52:145–149. [PubMed: 12204418]
- Cagniard B, Sotnikova TD, Gainetdinov RR, Zhuang X. The dopamine transporter expression level differentially affects responses to cocaine and amphetamine. *Journal of neurogenetics*. 2014; 28:112–121. [PubMed: 24673634]
- Carneiro AM, Ingram SL, Beaulieu JM, Sweeney A, Amara SG, Thomas SM, Caron MG, Torres GE. The multiple LIM domain-containing adaptor protein Hic-5 synaptically colocalizes and interacts with the dopamine transporter. *J Neurosci*. 2002; 22:7045–7054. [PubMed: 12177201]
- Carvelli L, McDonald PW, Blakely RD, Defelice LJ. Dopamine transporters depolarize neurons by a channel mechanism. *Proc Natl Acad Sci U S A*. 2004; 101:16046–16051. [PubMed: 15520385]
- Carvelli L, Blakely RD, DeFelice LJ. Dopamine transporter/syntaxin 1A interactions regulate transporter channel activity and dopaminergic synaptic transmission. *Proc Natl Acad Sci U S A*. 2008; 105:14192–14197. [PubMed: 18768815]

- Caudle WM, Richardson JR, Wang MZ, Taylor TN, Guillot TS, McCormack AL, Colebrooke RE, Di Monte DA, Emson PC, Miller GW. Reduced vesicular storage of dopamine causes progressive nigrostriatal neurodegeneration. *J Neurosci*. 2007; 27:8138–8148. [PubMed: 17652604]
- Cervinski MA, Foster JD, Vaughan RA. Syntaxin 1A regulates dopamine transporter activity, phosphorylation and surface expression. *Neuroscience*. 2010; 170:408–416. [PubMed: 20643191]
- D'Haene B, Vandesompele J, Hellemans J. Accurate and objective copy number profiling using real-time quantitative. *PCR Methods*. 2010; 50:262–270. [PubMed: 20060046]
- Foster JD, Pananusorn B, Vaughan RA. Dopamine transporters are phosphorylated on N-terminal serines in rat striatum. *J Biol Chem*. 2002; 277:25178–25186. [PubMed: 11994276]
- Foster JD, Cervinski MA, Gorentla BK, Vaughan RA. Regulation of the dopamine transporter by phosphorylation. *Handb Exp Pharmacol*. 2006:197–214.
- Fukushima S, Shen H, Hata H, Ohara A, Ohmi K, Ikeda K, Numachi Y, Kobayashi H, Hall FS, Uhl GR, Sora I. Methamphetamine-induced locomotor activity and sensitization in dopamine transporter and vesicular monoamine transporter 2 double mutant mice. *Psychopharmacology (Berl)*. 2007; 193:55–62. [PubMed: 17377774]
- Gainetdinov RR, Caron MG. Monoamine transporters: from genes to behavior. *Annu Rev Pharmacol Toxicol*. 2003; 43:261–284. [PubMed: 12359863]
- Gainetdinov RR, Jones SR, Fumagalli F, Wightman RM, Caron MG. Reevaluation of the role of the dopamine transporter in dopamine system homeostasis. *Brain Res Brain Res Rev*. 1998; 26:148–153. [PubMed: 9651511]
- Gainetdinov RR, Jones SR, Caron MG. Functional hyperdopaminergia in dopamine transporter knockout mice. *Biol Psychiatry*. 1999a; 46:303–311. [PubMed: 10435196]
- Gainetdinov RR, Wetsel WC, Jones SR, Levin ED, Jaber M, Caron MG. Role of serotonin in the paradoxical calming effect of psychostimulants on hyperactivity. *Science*. 1999b; 283:397–401. [PubMed: 9888856]
- Giros B, Jaber M, Jones SR, Wightman RM, Caron MG. Hyperlocomotion and indifference to cocaine and amphetamine in mice lacking the dopamine transporter. *Nature*. 1996; 379:606–612. [PubMed: 8628395]
- Gong S, Yang XW. Modification of bacterial artificial chromosomes (BACs) and preparation of intact BAC DNA for generation of transgenic mice. *Curr Protoc Neurosci*. 2005; 31:5.21.1–5.21.13.
- Gong S, Yang XW, Li C, Heintz N. Highly efficient modification of bacterial artificial chromosomes (BACs) using novel shuttle vectors containing the R6Kgamma origin of replication. *Genome Res*. 2002; 12:1992–1998. [PubMed: 12466304]
- Hastrup H, Karlin A, Javitch JA. Symmetrical dimer of the human dopamine transporter revealed by cross-linking Cys-306 at the extracellular end of the sixth transmembrane segment. *Proc Natl Acad Sci U S A*. 2001; 98:10055–10060. [PubMed: 11526230]
- Hastrup H, Sen N, Javitch JA. The human dopamine transporter forms a tetramer in the plasma membrane: cross-linking of a cysteine in the fourth transmembrane segment is sensitive to cocaine analogs. *J Biol Chem*. 2003; 278:45045–45048. [PubMed: 14519759]
- Hu YF, Caron MG, Sieber-Blum M. Norepinephrine transport-mediated gene expression in noradrenergic neurogenesis. *BMC Genomics*. 2009; 10:151. [PubMed: 19356247]
- Javitch JA, D'Amato RJ, Strittmatter SM, Snyder SH. Parkinsonism-inducing neurotoxin, N-methyl-4-phenyl-1,2,3,6-tetrahydropyridine: uptake of the metabolite N-methyl-4-phenylpyridine by dopamine neurons explains selective toxicity. *Proc Natl Acad Sci U S A*. 1985; 82:2173–2177. [PubMed: 3872460]
- Iversen LL. Role of transmitter uptake mechanisms in synaptic neurotransmission. *Br J Pharmacol*. 1971; 41:571–591. [PubMed: 4397129]
- Khoshbouei H, Sen N, Guptaroy B, Johnson L, Lund D, Gnegy ME, Galli A, Javitch JA. N-terminal phosphorylation of the dopamine transporter is required for amphetamine-induced efflux. *PLoS Biol*. 2004; 2:E78. [PubMed: 15024426]
- Lee SH, Kang SS, Son H, Lee YS. The region of dopamine transporter encompassing the 3rd transmembrane domain is crucial for function. *Biochem Biophys Res Commun*. 1998; 246:347–352. [PubMed: 9610361]

- Lee FJ, Liu F, Pristupa ZB, Niznik HB. Direct binding and functional coupling of alpha-synuclein to the dopamine transporters accelerate dopamine-induced apoptosis. *FASEB J.* 2001; 15:916–926. [PubMed: 11292651]
- Lee KH, Kim MY, Kim DH, Lee YS. Syntaxin 1A and receptor for activated C kinase interact with the N-terminal region of human dopamine transporter. *Neurochem Res.* 2004; 29:1405–1409. [PubMed: 15202772]
- Lee FJ, Pei L, Moszczynska A, Vukusic B, Fletcher PJ, Liu F. Dopamine transporter cell surface localization facilitated by a direct interaction with the dopamine D2 receptor. *EMBO J.* 2007; 26:2127–2136. [PubMed: 17380124]
- Livak KJ, Schmittgen TD. Analysis of relative gene expression data using real-time quantitative PCR and the 2(-delta delta C(T)) method. *Methods.* 2001; 25:402–408. [PubMed: 11846609]
- Melikian HE. Neurotransmitter transporter trafficking: endocytosis, recycling, and regulation. *Pharmacol Ther.* 2004; 104:17–27. [PubMed: 15500906]
- Melikian HE, Buckley KM. Membrane trafficking regulates the activity of the human dopamine transporter. *J Neurosci.* 1999; 19:7699–7710. [PubMed: 10479674]
- Miranda M, Sorkina T, Grammatopoulos TN, Zawada WM, Sorkin A. Multiple molecular determinants in the carboxyl terminus regulate dopamine transporter export from endoplasmic reticulum. *J Biol Chem.* 2004; 279:30760–30770. [PubMed: 15128747]
- Miranda M, Dionne KR, Sorkina T, Sorkin A. Three ubiquitin conjugation sites in the amino terminus of the dopamine transporter mediate protein kinase C-dependent endocytosis of the transporter. *Mol Biol Cell.* 2007; 18:313–323. [PubMed: 17079728]
- Moron JA, Zakharova I, Ferrer JV, Merrill GA, Hope B, Lafer EM, Lin ZC, Wang JB, Javitch JA, Galli A, Shippenberg TS. Mitogen-activated protein kinase regulates dopamine transporter surface expression and dopamine transport capacity. *J Neurosci.* 2003; 23:8480–8488. [PubMed: 13679416]
- Mortensen OV, Amara SG. Dynamic regulation of the dopamine transporter. *Eur J Pharmacol.* 2003; 479:159–170. [PubMed: 14612147]
- Moszczynska A, Saleh J, Zhang H, Vukusic B, Lee FJ, Liu F. Parkin disrupts the alpha-synuclein/dopamine transporter interaction: consequences toward dopamine-induced toxicity. *J Mol Neurosci.* 2007; 32:217–227. [PubMed: 17873367]
- Nelson N. The family of Na⁺/Cl⁻-neurotransmitter transporters. *J Neurochem.* 1998; 71:1785–1803. [PubMed: 9798903]
- Pfaffl MW. A new mathematical model for relative quantification in real-time RT-PCR. *Nucleic Acids Res.* 2001; 29:e45. [PubMed: 11328886]
- Rao A, Richards TL, Simmons D, Zahniser NR, Sorkin A. Epitope-tagged dopamine transporter knock-in mice reveal rapid endocytic trafficking and filopodia targeting of the transporter in dopaminergic axons. *FASEB J.* 2012; 26:1921–1933. [PubMed: 22267337]
- Rao A, Sorkin A, Zahniser NR. Mice expressing markedly reduced striatal dopamine transporters exhibit increased locomotor activity, dopamine uptake turnover rate and cocaine responsiveness. *Synapse.* 2013; 67:668–677. [PubMed: 23564231]
- Rickhag M, Hansen FH, Sorensen G, Strandfelt KN, Andresen B, Gotfryd K, Madsen KL, Vestergaard-Klewe I, Ammendrup-Johnsen I, Eriksen J, Newman AH, Fuchtbauer EM, Gomeza J, Woldbye DP, Wortwein G, Gether U. A C-terminal PDZ domain-binding sequence is required for striatal distribution of the dopamine transporter. *Nat Commun.* 2013; 4:1580. [PubMed: 23481388]
- Salahpour A, Medvedev IO, Beaulieu JM, Gainetdinov RR, Caron MG. Local knockdown of genes in the brain using small interfering RNA: a phenotypic comparison with knockout animals. *Biol Psychiatry.* 2007; 61:65–69. [PubMed: 16712807]
- Salahpour A, Ramsey AJ, Medvedev IO, Kile B, Sotnikova TD, Holmstrand E, Ghisi V, Nicholls PJ, Wong L, Murphy K, Sesack SR, Wightman RM, Gainetdinov RR, Caron MG. Increased amphetamine-induced hyperactivity and reward in mice overexpressing the dopamine transporter. *Proc Natl Acad Sci U S A.* 2008; 105:4405–4410. [PubMed: 18347339]
- Salamone JD, Correa M. The mysterious motivational functions of mesolimbic dopamine. *Neuron.* 2012; 76:470–485. [PubMed: 23141060]

- Schmittgen TD, Livak KJ. Analyzing real-time PCR data by the comparative C(T) method. *Nat Protoc.* 2008; 3:1101–1108. [PubMed: 18546601]
- Schultz W. Multiple dopamine functions at different time courses. *Annu Rev Neurosci.* 2007; 30:259–288. [PubMed: 17600522]
- Shepherd CT, Moran Lauter AN, Scott MP. Determination of transgene copy number by real-time quantitative PCR. *Methods Mol Biol.* 2009; 526:129–134. [PubMed: 19378009]
- Sorkina T, Miranda M, Dionne KR, Hoover BR, Zahniser NR, Sorkin A. RNA interference screen reveals an essential role of Nedd4-2 in dopamine transporter ubiquitination and endocytosis. *J Neurosci.* 2006; 26:8195–8205. [PubMed: 16885233]
- Sorkina T, Richards TL, Rao A, Zahniser NR, Sorkin A. Negative regulation of dopamine transporter endocytosis by membrane-proximal N-terminal residues. *J Neurosci.* 2009; 29:1361–1374. [PubMed: 19193883]
- Torres GE. The dopamine transporter proteome. *J Neurochem.* 2006; 97 (Suppl 1):3–10. [PubMed: 16635244]
- Torres GE, Yao WD, Mohn AR, Quan H, Kim KM, Levey AI, Staudinger J, Caron MG. Functional interaction between monoamine plasma membrane transporters and the synaptic PDZ domain-containing protein PICK1. *Neuron.* 2001; 30:121–134. [PubMed: 11343649]
- Torres GE, Carneiro A, Seamans K, Fiorentini C, Sweeney A, Yao WD, Caron MG. Oligomerization and trafficking of the human dopamine transporter. Mutational analysis identifies critical domains important for the functional expression of the transporter. *J Biol Chem.* 2003a; 278:2731–2739. [PubMed: 12429746]
- Torres GE, Gainetdinov RR, Caron MG. Plasma membrane monoamine transporters: structure, regulation and function. *Nat Rev Neurosci.* 2003b; 4:13–25. [PubMed: 12511858]
- Tye KM, Mirzabekov JJ, Warden MR, Ferenczi EA, Tsai HC, Finkelstein J, Kim SY, Adhikari A, Thompson KR, Andalman AS, Gunaydin LA, Witten IB, Deisseroth K. Dopamine neurons modulate neural encoding and expression of depression-related behaviour. *Nature.* 2013; 493:537–541. [PubMed: 23235822]
- Vaughan RA. Phosphorylation and regulation of psychostimulant-sensitive neurotransmitter transporters. *J Pharmacol Exp Ther.* 2004; 310:1–7. [PubMed: 15064332]
- Vaughan RA, Huff RA, Uhl GR, Kuhar MJ. Protein kinase C-mediated phosphorylation and functional regulation of dopamine transporters in striatal synaptosomes. *J Biol Chem.* 1997; 272:15541–15546. [PubMed: 9182590]
- Zhuang X, Oosting RS, Jones SR, Gainetdinov RR, Miller GW, Caron MG, Hen R. Hyperactivity and impaired response habituation in hyperdopaminergic mice. *Proc Natl Acad Sci U S A.* 2001; 98:1982–1987. [PubMed: 11172062]

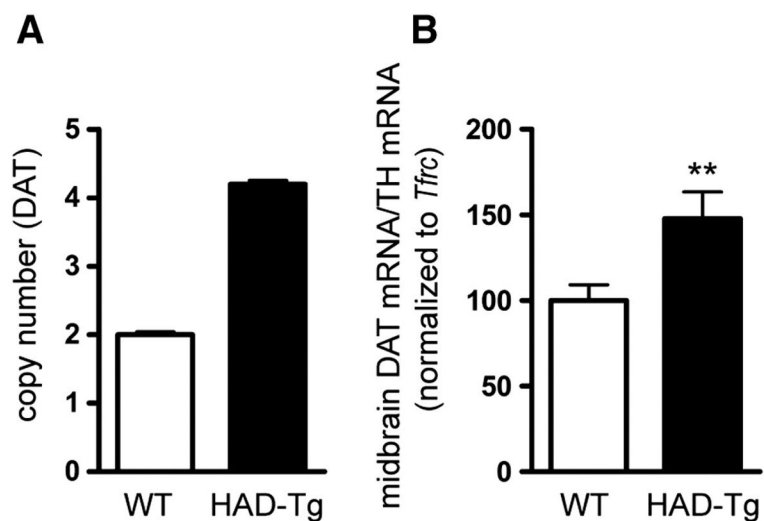


Fig. 1.

Gene copy number and mRNA levels. (A) Quantitative PCR (q-PCR) of genomic DNA indicates that two copies of the HA-DAT transgene are incorporated into the genome, producing a total of 4 copies of the locus. (B) q-PCR of midbrain cDNA demonstrates a 47% increase in DAT mRNA in transgenic mice ($n = 10$) as compared to wildtype ($n = 13$). Mean \pm SEM. ** $p < 0.01$.

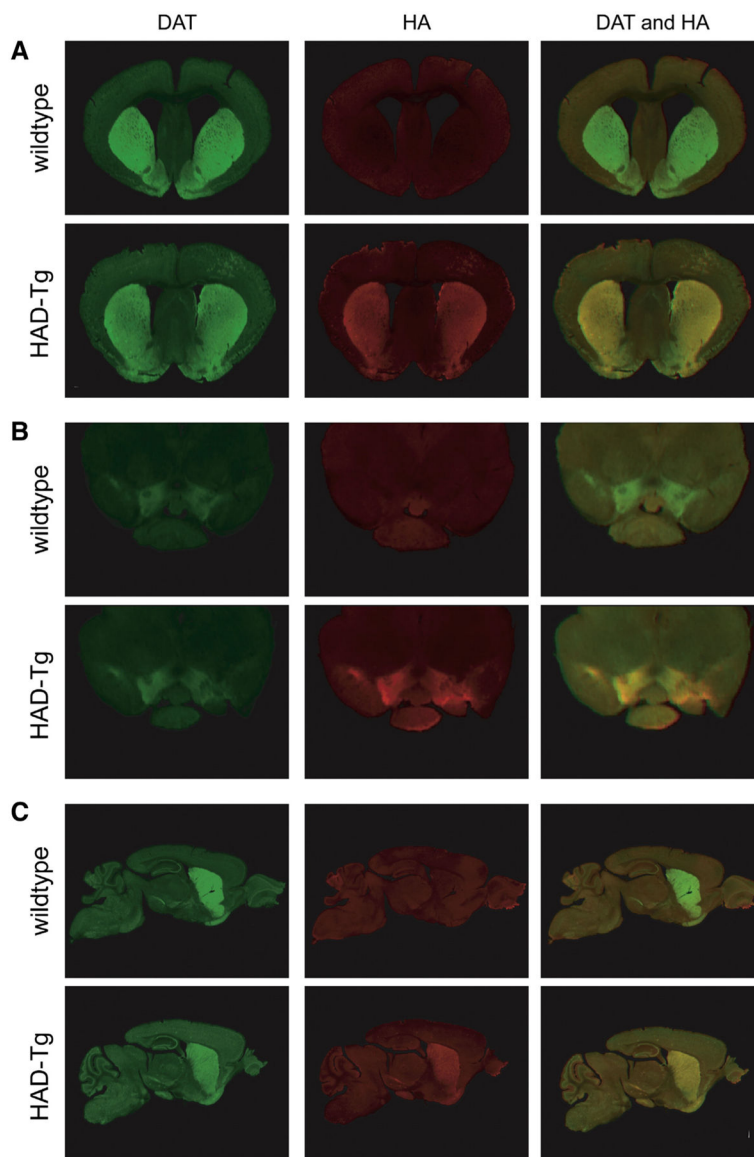
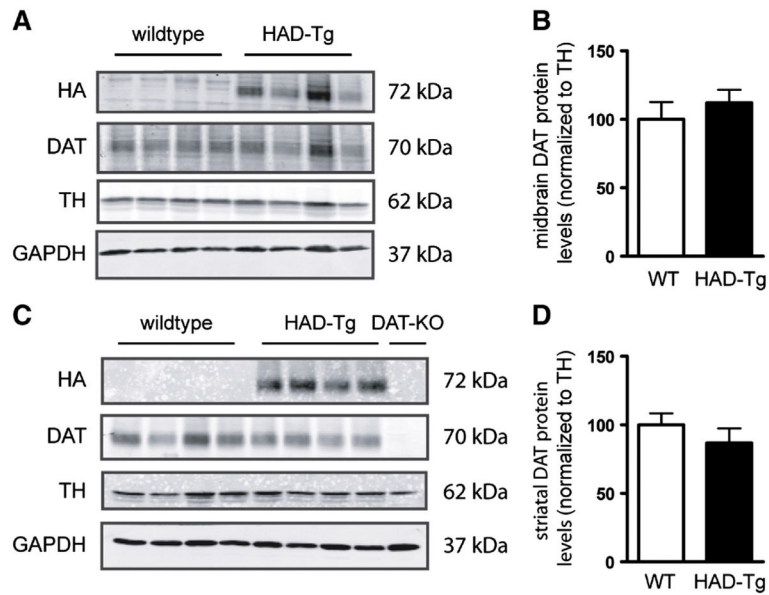


Fig. 2. Expression pattern of HA-tagged DAT using immunofluorescence. Co-labeling of DAT protein (green) and HA protein (red) in coronal sections of the striatum (A) and midbrain (B). Where both DAT and HA are co-expressed, regions appear yellow. In transgenic mice, HA and DAT are shown to be co-expressed throughout the nigrostriatal pathway, as seen in sagittal sections containing both the midbrain and striatum (C).

**Fig. 3.**

DAT protein expression in midbrain and striatum of HAD-Tg mice. Densitometric analyses of western blots of HA-tagged and endogenous DAT in HAD-Tg and wildtype (WT) mice. Midbrain (A) and striatum (C) western blot using anti-DAT and anti-HA antibodies. Anti-TH and anti-GAPDH antibodies are used as loading controls. Quantification of signal from DAT antibody normalized to TH levels (B, D). N = 4 DAT-KO striatal protein was included to confirm antibody selectivity to DAT.

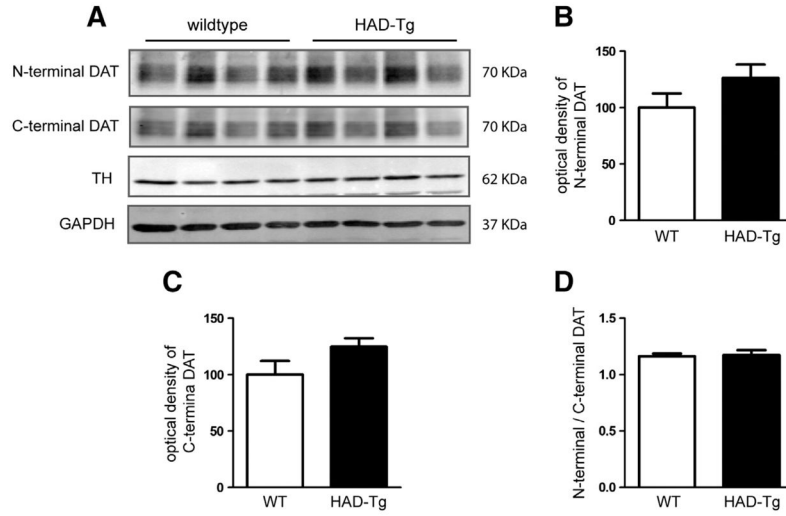


Fig. 4. Western blot using antibodies that recognize the N- and C-terminus antibodies of DAT. (A) Wildtype (WT) and transgenic striatal protein (HAD-Tg) probed with the N-terminal antibody or a C-terminal antibody (n = 4 for both genotypes). (B) Densitometric analysis of the N-terminal anti-DAT antibody. (C) Densitometric analysis of the C-terminal anti-DAT antibody. (D) The ratio of N-terminal to C-terminal DAT (optical density) in WT compared to HAD-Tg + samples. For all densitometric analyses, the optical density of N- and C-terminal DAT is normalized to the optical density of TH, and HAD-Tg DAT levels are presented relative to WT. Mean \pm SEM.

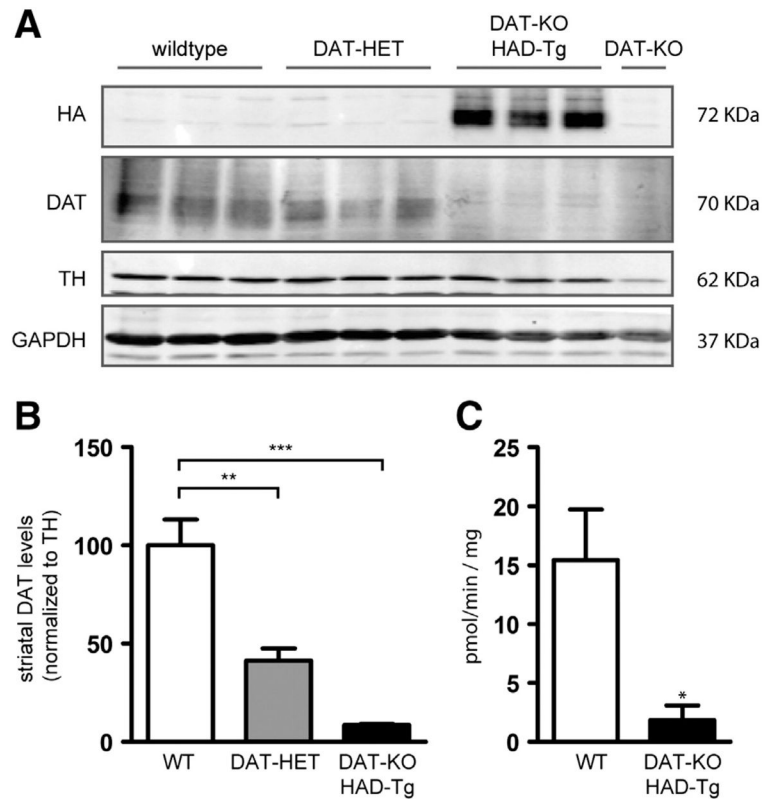


Fig. 5. Striatal DAT protein levels in HAD-Tg mice that lack endogenous DAT. (A) Representative western blot showing DAT protein levels in wildtype mice (WT, $n = 3$), heterozygous (DAT-HET, $n = 3$) mice and HAD-Tg mice that lack endogenous DAT (DAT-KO/HAD-Tg, $n = 3$). A DAT-KO sample is shown as a control for immunoreactivity ($n = 1$). (B) Densitometric analysis of DAT protein levels. Mean \pm SEM ($p = 0.01$, **; $p = 0.001$, ***) ($F_{2,6} = 30.40$, $p = 0.0007$, one-way ANOVA). (C) Uptake of $^3\text{H}[\text{DA}]$ into striatal synaptosomes of WT and DAT-KO/HAD-Tg mice. Mean values for V_{max} shown (pmol per min per mg protein). The average V_{max} of DAT-KO controls was deducted from all WT and DAT-KO/HAD-Tg values ($n = 3$ for both genotypes). Mean \pm SEM, $p = 0.038$.

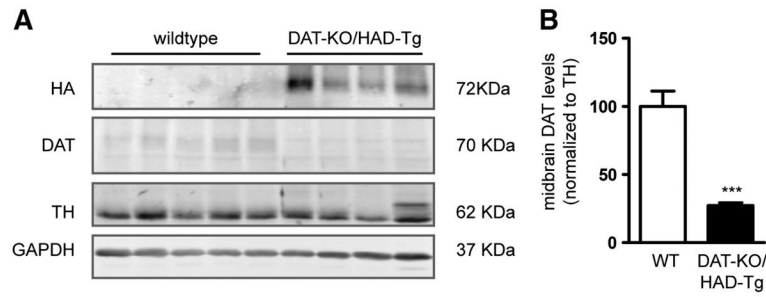


Fig. 6. Midbrain DAT protein levels in HAD-Tg mice that lack endogenous DAT. (A) Representative western blot showing DAT protein levels in midbrain of wildtype mice (WT, n = 4) and HAD-Tg mice lacking endogenous DAT (DAT-KO/HAD-Tg, n = 4). (B) Densitometric analysis of DAT protein levels normalized to TH. Mean \pm SEM, p = 0.001.

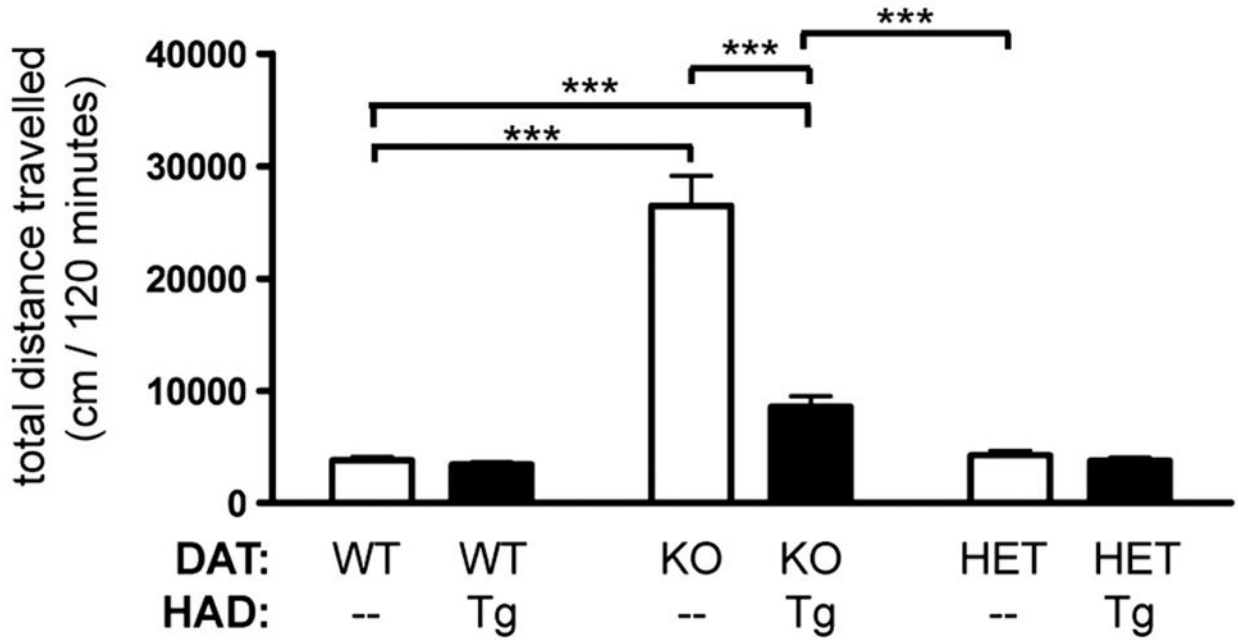


Fig. 7.

Rescue of DAT-knockout hyperactivity by HA-tagged DAT. Total distance traveled (cm) in 120 min in a novel environment. WT (n = 18); HAD Tg (n = 13); DAT-KO (n = 18); DAT-KO/HAD Tg (n = 10); DAT-HET (n = 15); DAT-HET/HAD Tg (n = 16). Two-way ANOVA shows effect of DAT-KO genotype, $F_{2,84} = 61.53$, $p < 0.0001$. Genotype \times genotype interaction is significant ($F_{2,84} = 24.90$, $p = 0.0003$). Post-hoc Bonferroni comparing DAT-KO to DAT-KO/HAD-Tg, $p < 0.001$. t-Test comparing WT to DAT-KO, $p < 0.001$. t-Test comparing WT to DAT-KO/HAD-Tg, $p < 0.001$. t-Test comparing DAT-KO/HAD-Tg to DAT-HET, $p = 0.0001$.

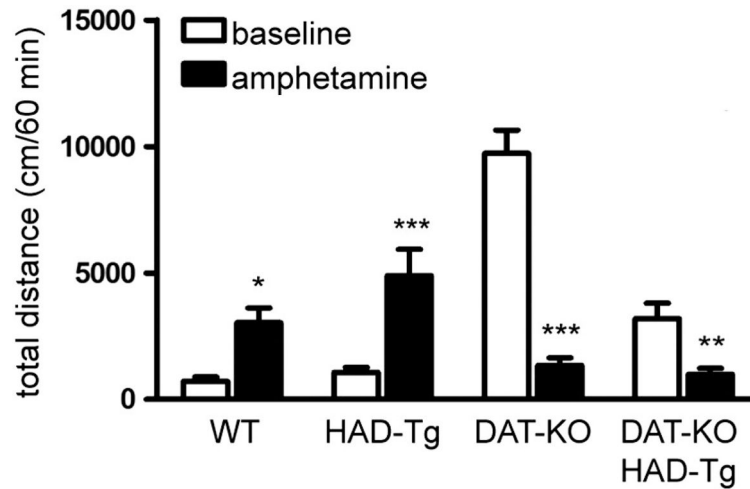


Fig. 8.

Locomotor response to amphetamine. Total distance traveled (cm) in the 60 min prior to injection (baseline) and 60 min post-injection of 2.0 mg/kg amphetamine (amphetamine). WT (n = 8); HAD-Tg (n = 8); DAT-KO (n = 8); DAT-KO/HAD-Tg (n = 13). Two-way ANOVA shows a significant effect of genotype ($F_{3,66} = 15.77$, $p < 0.0001$) and of drug ($F_{1,66} = 17.12$, $p = 0.01$). In addition, a significant genotype \times drug interaction was observed ($F_{3,66} = 39.59$, $p < 0.0001$). Mean \pm SEM (Bonferroni post-hoc, $p = 0.015$, *, $p = 0.01$, **, $p = 0.001$, ***).

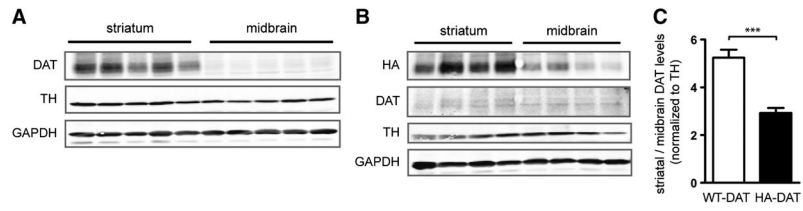


Fig. 9. Western blot of DAT levels in striatum and midbrain of WT and DAT-KO/HAD-Tg animals. (A) Western blot of striatum and midbrain protein from wildtype (n = 5). (B) Western blot of striatum and midbrain protein from HA-DAT transgenic mice lacking endogenous DAT (DAT-KO/HAD-Tg) (n = 4). (C) Densitometric analysis of the striatum:midbrain ratio of DAT protein normalized to TH. Mean \pm SEM (t-test, $p < 0.001$, ***).

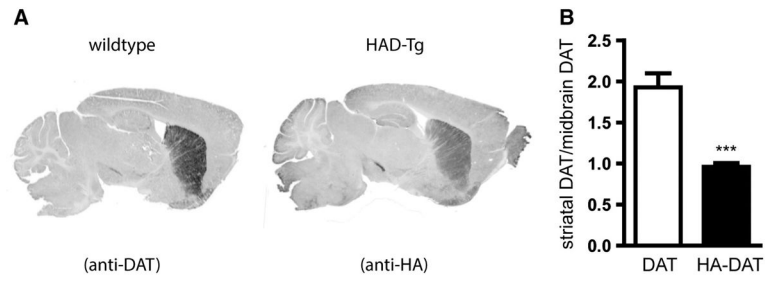


Fig. 10.

Immunofluorescent staining to detect distribution of DAT and HA-tagged DAT.

Immunofluorescence detected by Licor imager and converted to grayscale. (A)

Representative image of immunofluorescence staining for DAT in WT sections and for HA

in HAD-Tg sections. (B) Densitometric analysis of the striatum:midbrain ratio of DAT

protein in WT slices and of HA-DAT in HAD-Tg slices. n = 5 per genotype. Mean ± SEM (t-test, p < 0.001, ***).